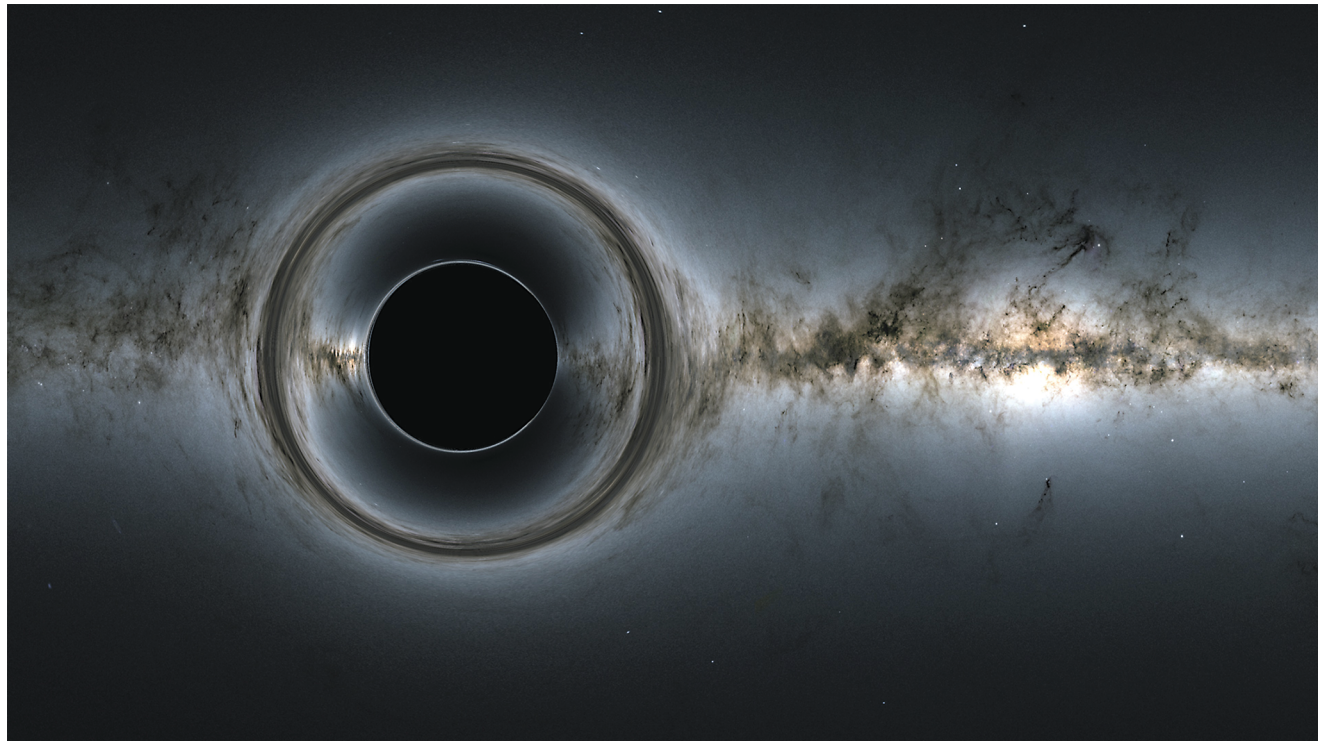


---

# Trapped Surfaces, Topology of Black Holes, and the Positive Mass Theorem



*Lan-Hsuan Huang and Dan A. Lee*

---

## 1. Introduction

Albert Einstein's theory of general relativity, first published in 1915, successfully unified special relativity with gravity and led to many predictions that have since been verified, marking one of the greatest triumphs of 20th century physics. Perhaps one of the most sensational features of the theory is the concept of a black hole—a region from which even light cannot escape. But what is a black hole,

precisely? Do black holes really exist in nature? What do black holes have to do with mathematics?

These questions and others have been pondered by generations of researchers. The 2020 Nobel Prize in Physics was awarded to mathematical physicist Roger Penrose for his "discovery that black hole formation is a robust prediction of the general theory of relativity," and to astrophysicists Reinhard Genzel and Andrea Ghez for their "discovery of a supermassive compact object at the centre of our galaxy." Although the very first nontrivial solution to Einstein's equations ever discovered—the Schwarzschild spacetime—describes a black hole, many physicists, including Einstein, believed that black hole regions might only be present in highly symmetric solutions that were not realistic enough to describe nature. Penrose's seminal 1965 paper [Pen65] implied that the singular behavior associated with black holes persists even without

---

*Lan-Hsuan Huang is a professor of mathematics at the University of Connecticut. Part of the work is supported by NSF CAREER DMS-1452477 and grant DMS-2005588. Her email address is lan-hsuan.huang@uconn.edu.*

*Dan A. Lee is an associate professor of mathematics at Queens College and the CUNY Graduate Center. His email address is dan.lee@qc.cuny.edu.*

*Communicated by Notices Associate Editor Daniela De Silva.*

*For permission to reprint this article, please contact:*

*reprint-permission@ams.org.*

*DOI: <https://doi.org/10.1090/noti2453>*

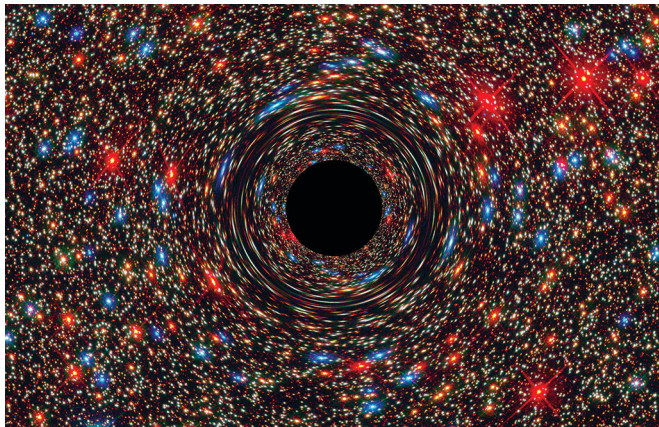


**Figure 1.** This computer-simulated image shows a supermassive black hole at the center of a galaxy. The black region represents a snapshot of the event horizon of the black hole. Light from background stars is stretched and distorted due to the strong gravity of the black hole.

symmetry, which was enough to convince many that black hole formation was a real physical phenomenon. But perhaps just as importantly, Penrose revolutionized the study of general relativity by introducing global differential geometric and topological methods, in contrast to the more calculation-based approaches of the past.

Also starting in the 1960s, the study of quasars eventually led astrophysicists to hypothesize that there were black holes at the centers of most galaxies, including our own galaxy, the Milky Way. It is difficult to directly observe something that cannot emit light, but starting in the 1990s, separate teams led by Genzel and Ghez began making detailed observations of the movements of stars near the center of the Milky Way, and after decades of collecting increasingly accurate data, we can now be confident that those movements are consistent with the existence of a black hole whose mass is 4.3 million times that of our Sun [EG96, GKMB98]. See Figure 2.

Even more recently, in 2019, the Event Horizon Telescope—an international collaboration linking radio telescopes across the globe—treated us to spectacular



**Figure 2.** The W. M. Keck Observatory is a two-telescope astronomical observatory near the summit of Mauna Kea in Hawaii. Starting in the 1990s, Ghez and her team used these telescopes and adaptive optics systems to track multiple stars orbiting the center of our galaxy.

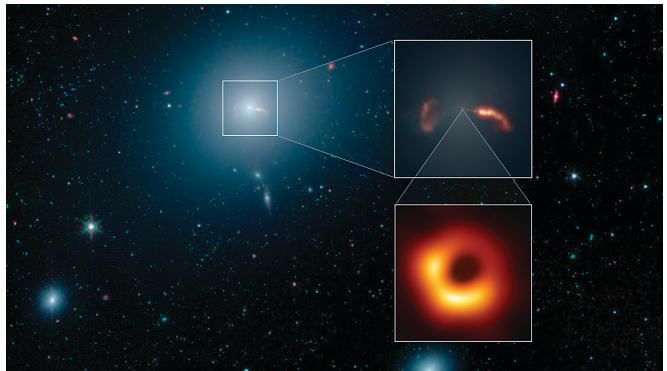


**Figure 3.** This image shows the elliptical galaxy Messier 87. The right top inset gives a close-up of two shockwaves created by a jet emanating from the galaxy's supermassive black hole. The right bottom inset shows an image of that black hole produced by the Event Horizon Telescope [Eve19].

pictures of the black hole (or rather, the “shadow” created by it) at the heart of Messier 87, an elliptical galaxy 55 million light-years from Earth. See Figure 3.

In this article we provide an exposition of Penrose’s groundbreaking concepts of trapped surfaces and marginally outer trapped surfaces (MOTS), and some of their applications. Specifically, we will discuss Stephen Hawking’s result on the topology of black holes and some recent developments on the positive mass theorem that go back to the work of Richard Schoen and Shing-Tung Yau. The study of MOTS gives an effective way to understand some properties of black holes and turns out to have many analogies with the study of minimal surfaces. The theory of minimal surfaces is a mathematically rich topic with a long history that goes back to Lagrange’s work in the 18th century. Minimal surfaces also have many applications to such diverse fields as architecture, biology, and engineering, in addition to general relativity. See Figure 4. Exploring the intriguing connections between MOTS and minimal surfaces has led to fruitful developments in both general relativity and differential geometry.

## 2. Trapped Surfaces

In this article our basic setting is a 4-dimensional spacetime, representing one time dimension and three spatial dimensions, and since we would like to describe an (effectively) isolated gravitational system, such as a galaxy, we assume that this spacetime is asymptotic to the trivial flat spacetime, which is usually called the Minkowski spacetime, near “infinity.” A rigorous general mathematical definition of a black hole is quite technical, but roughly speaking, when we refer to the *black hole region* of a spacetime, we mean a region that has the property that light rays emanating from the black hole region can never reach its complement, while from every point of the complement, one should be able to “escape to infinity” by following a

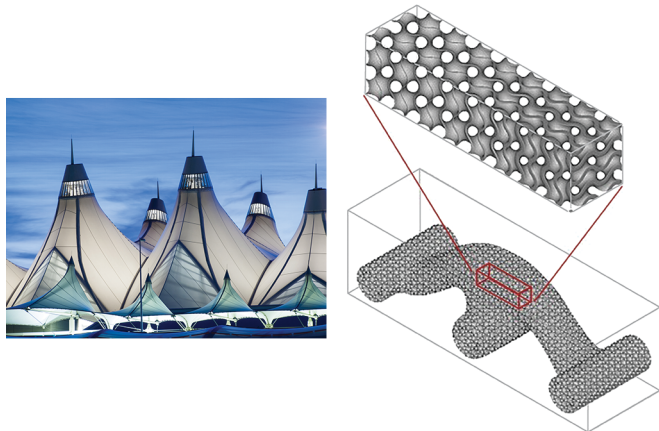


**Figure 4.** Left: The roof of the Denver International Airport is a tensioned fabric structure that employs double-curved minimal surfaces. Right: Triply periodic minimal surfaces are used in industry as cost-effective functional components to produce high-complexity customized structures via 3D printing technology.

light ray. The boundary of the black hole region is called the *event horizon*. Given a spatial 3-dimensional “snapshot in time”  $M$  in our spacetime, we would like to understand which points in  $M$  lie inside the black hole, but unfortunately, since the black hole region can only be technically defined in terms of global properties of the spacetime, it is impossible to tell whether or not a given point in  $M$  lies inside the black hole without complete knowledge of the long-term spacetime future of  $M$ .

Penrose’s concept of a trapped surface offers us an accessible way to understand the location of a black hole without knowing its long-term future: Given a 2-surface  $\Sigma$  in spacetime, imagine shooting a light ray from each point of  $\Sigma$ , and then define  $\Sigma_t$  to be the surface obtained by following these light rays for parameter-time  $t$ , so that  $\Sigma_t$  can be thought of as a “shell of light” emanating from  $\Sigma$ . (Note that we should not think of this  $t$  as actual “time” since light does not experience passage of time.) We typically expect that if we shoot these light rays inward, the area of  $\Sigma_t$  will decrease in  $t$ , and that if we shoot them outward, the area of  $\Sigma_t$  will increase, as is the case for a standard sphere in the Minkowski spacetime. However, in the presence of strong gravity, it is possible for the family of outgoing light shells to have decreasing area forms at each point of  $\Sigma$ , and in this case we say that  $\Sigma$  is an (*outer*) *trapped surface*. See Figure 5. Meanwhile, a *marginally outer trapped surface* (*or MOTS*) refers to the borderline case in which the area forms at each point are unchanging to first-order in  $t$ .

Penrose’s famed singularity theorem states that under certain physically reasonable assumptions, the existence of a closed trapped surface implies that there is a light ray emanating from the trapped surface that eventually runs into a singularity. Intuitively, the behavior of a trapped

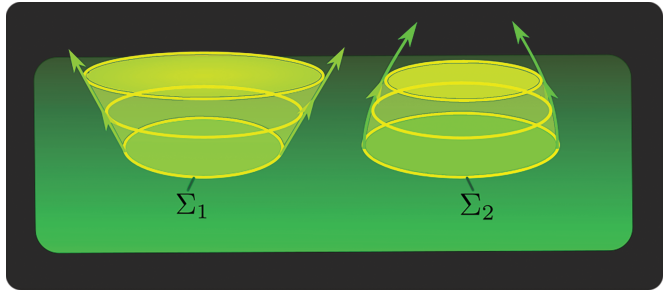


**Figure 5.** Typically, the outgoing “light shell” has increasing area form as it exits the surface, as shown for the surface  $\Sigma_1$ . Meanwhile, for the trapped surface  $\Sigma_2$ , the area form is decreasing.

surface feels a bit like saying that even though the light rays are “directed outward,” they are still “moving inward,” which vaguely captures the idea of light not being able to “escape.” Because of this heuristic and Penrose’s singularity theorem, physicists often associate trapped surfaces with the existence of black holes, and in fact, under certain global hypotheses, one can even prove that trapped surfaces must lie inside the black hole region. Because of this relationship, the (*weakly*) *trapped region* of  $M$ , which we define to be the region of  $M$  enclosed by either trapped surfaces or MOTS in  $M$ , can be thought of as a simpler stand-in for the intersection of  $M$  with the black hole region, and the *apparent horizon* of  $M$ , which we define to be the boundary of the trapped region of  $M$ , can be thought of as a simpler stand-in for the intersection of  $M$  with the event horizon. The advantage of these concepts is that the trapped region and apparent horizon are entirely determined by data along the spatial 3-dimensional “snapshot in time”  $M$ .

### 3. Spacetime Geometry

Since we want to consider 4-dimensional spacetimes but without a uniquely determined “time coordinate,” the natural setting of general relativity is a 4-manifold. A Lorentzian metric  $\mathbf{g}$  on a 4-manifold  $N$  defines an inner product with signature  $(-, +, +, +)$  on each tangent space of  $N$ , smoothly depending on the base point. This means that at each point of  $N$ , there is an orthogonal basis of tangent vectors  $\{e_0, e_1, e_2, e_3\}$  such that  $\mathbf{g}(e_0, e_0) = -1$  and  $\mathbf{g}(e_i, e_i) = +1$  for  $i = 1, 2, 3$ . So if a tangent vector  $v$  is given by  $(v^0, v^1, v^2, v^3)$  when written in this basis, then  $\mathbf{g}(v, v) = -(v^0)^2 + (v^1)^2 + (v^2)^2 + (v^3)^2$ . If one thinks of Riemannian geometry as being locally modeled on the Euclidean metric  $ds^2 = dx^2 + dy^2 + dz^2$ , one can analogously think of Lorentzian geometry as being locally modeled on the Minkowski metric  $ds^2 = -dt^2 + dx^2 + dy^2 + dz^2$ . Special relativity is essentially the physics of Minkowski geometry, so the reason why a Lorentzian manifold is the natural setting for general relativity is that the theory should be locally modeled on special relativity. Moreover, we

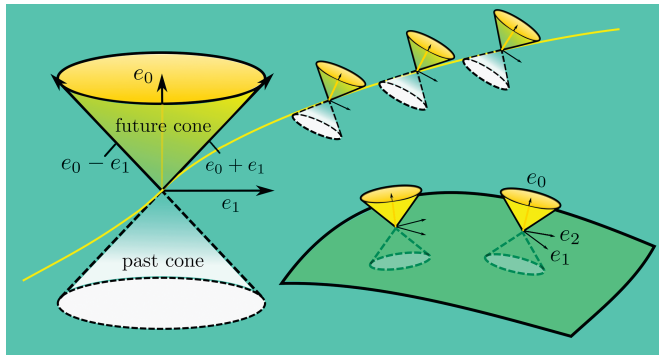


**Figure 6.** At the tangent space of each point, one can define the future and past light cones. Two future null vectors  $e_0 + e_1$  and  $e_0 - e_1$  are given. The yellow curve is null as its tangent vector is null at each point. The submanifold at the bottom-right is spacelike because its tangent vectors are spacelike at each point.

will often implicitly assume that  $\mathbf{g}$  is asymptotic to the Minkowski metric in some sense.

For any tangent vector  $v$  of  $N$ , we call it *timelike* if  $\mathbf{g}(v, v) < 0$ , *null* if  $\mathbf{g}(v, v) = 0$ , and *spacelike* if  $\mathbf{g}(v, v) > 0$ . So for example,  $e_0$  is timelike,  $e_1$  is spacelike, and  $e_0 + e_1$  is null. The null vectors form a double cone which separates the timelike vectors from the spacelike ones. A *spacetime* is a Lorentzian 4-manifold  $(N, \mathbf{g})$  equipped with a globally defined unit timelike vector field, which we may select as our  $e_0$  at every point. This choice allows us to further distinguish between *future* null or timelike vectors, which lie on or above the upper half of the null cone, and *past* null or timelike vectors, which lie on or below the lower half of the null cone.

A submanifold of  $N$  is called *spacelike* if all of its tangent vectors are spacelike, or equivalently, if  $\mathbf{g}$  induces a Riemannian metric on it. In particular, we define a *spacelike slice* of  $N$  to be a 3-dimensional spacelike hypersurface  $M$ , which is what we earlier referred to as a “snapshot in time.” The induced Riemannian metric  $g$  and the second fundamental form<sup>1</sup>  $k$  of a spacelike slice  $M$  can largely capture the spacetime geometry along  $M$ , and we will refer to  $(M, g, k)$  as an *initial data set*. A curve is called *null* (or *timelike*) if its tangent vector is *null* (or *timelike*) at each point. See Figure 6. As in Riemannian geometry, a Lorentzian metric  $\mathbf{g}$  gives us a concept of “straight lines,” which we call *geodesics*. The path of a *light ray* traces out a future null geodesic in the spacetime, while a massive test particle will trace out a future timelike geodesic. A test particle that traces out a spacelike geodesic would travel faster than the speed of light, and thus it is unphysical.

Einstein’s equations demand that certain “curvatures” of  $\mathbf{g}$  must be equal to the stress-energy tensor, which

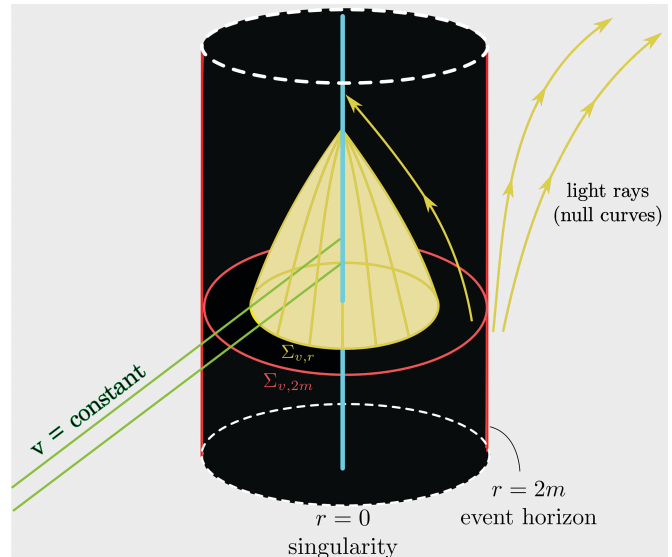


**Figure 7.** The Schwarzschild metric in the ingoing Eddington-Finkelstein coordinates (one space dimension suppressed). Any light ray that starts at a point where  $r < 2m$  will crash into the  $r = 0$  singularity. The surfaces  $\Sigma_{v,r}$  defined by constant  $v, r$  coordinates are trapped surfaces whenever  $r < 2m$ , and they are MOTS when  $r = 2m$ .

describes the distribution of energy in the spacetime.<sup>2</sup> One can view these equations as a complicated nonlinear system of partial differential equations on  $\mathbf{g}$ , with the stress-energy tensor as a source term. An initial data set  $(M, g, k)$  may be regarded as Cauchy data for this system of partial differential equations, as explicated by the fundamental work of Yvonne Choquet-Bruhat on well-posedness of the Einstein equations.

As alluded to earlier, the Schwarzschild metrics were the first nontrivial solutions to be discovered with source term equal to zero. In one particular choice of coordinates, the *Schwarzschild metric of mass  $m$*  can be written as

$$\mathbf{g}_m = -\left(1 - \frac{2m}{r}\right)dv^2 + 2dvdr + r^2d\Omega^2,$$

which is a smooth Lorentzian metric on  $\mathbb{R} \times (0, \infty) \times S^2$ , where  $v \in \mathbb{R}$ ,  $r \in (0, \infty)$ , and  $d\Omega^2$  is the standard Riemannian metric on the sphere  $S^2$ . In this spacetime, one can show that a light ray emanating from within the region  $r \leq 2m$  can never enter the region  $r > 2m$ , while any point in the region  $r > 2m$  can be connected to “infinity” by a light ray. Or in other words, the region  $r \leq 2m$  is a black hole region, with its boundary  $r = 2m$  as the event horizon. It is also a fact that as  $r$  approaches zero, the metric becomes singular there in the sense that the curvature blows up, and moreover, any light ray (or massive test

<sup>1</sup>The second fundamental form of  $M \subset (N, \mathbf{g})$  is defined to be the tangential part of  $\nabla_{\mathbf{g}} \mathbf{n}$  where  $\mathbf{n}$  is the future unit normal of  $M$ .

<sup>2</sup>Specifically, the curvatures referred to here are the Einstein tensor of  $\mathbf{g}$ , defined to be  $\mathbf{G} = \mathbf{Ric} - \frac{1}{2}\mathbf{R}\mathbf{g}$  where  $\mathbf{Ric}$  and  $\mathbf{R}$  are the Ricci and scalar curvatures of  $\mathbf{g}$ , respectively.

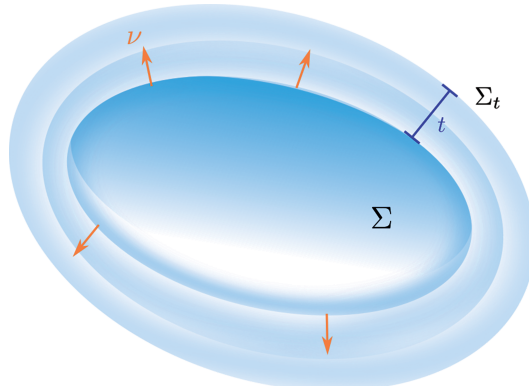


**Figure 8.** Parallel surfaces of distance  $t$  away from  $\Sigma$  in the direction  $\nu$  are shown. Positive mean curvature of  $\Sigma$  is characterized by the property that the area of  $\Sigma_t$  increases in  $t$  for small  $t$ .

particle) starting at a point where  $r < 2m$  will inevitably crash into this singularity. See Figure 7.

#### 4. Variations of Surface Area

Earlier we described trapped surfaces in terms of decreasing area forms of “light shells.” Here we will make that precise, but first we discuss the simpler concept of varying the area form of a surface  $\Sigma$  in a Riemannian 3-manifold  $(M, g)$ . Suppose  $\nu$  is a unit normal vector on  $\Sigma$ , which we will regard as the “outward” direction (regardless of whether  $\Sigma$  separates  $M$  into an “outside” and “inside”), and let  $\Phi_t$  be a family of diffeomorphisms on  $M$  with  $\Phi_0$  equal to the identity. Then  $\Sigma_t := \Phi_t(\Sigma)$  defines a family of surfaces, sometimes called variations of  $\Sigma$ , whose first-order variation vector field  $X$  along  $\Sigma$  is defined by  $X(p) := \frac{\partial}{\partial t} \Big|_{t=0} \Phi_t(p)$  for each  $p \in \Sigma$ . Let us consider *outward normal variations*, which are those for which  $X = e^u \nu$  along  $\Sigma$ , for some smooth function  $u$ .

One simple variation of  $\Sigma$  is the family of parallel surfaces, obtained by taking  $\Phi_t(p) = \exp_p(tv)$  for small  $t$ , at each  $p \in \Sigma$ , where  $\exp_p$  is the exponential map at  $p$ . This just means that  $\Phi_t(p)$  is obtained by starting at  $p$ , and then moving along the geodesic pointing in the  $\nu$  direction for  $t$  units of arclength. These are called parallel surfaces because  $\Sigma_t$  will be exactly a (signed) distance  $t$  away from  $\Sigma$  in the  $\nu$  direction (for small enough  $t$ ). For this family, the first-order variation  $X$  is just  $\nu$ , and this family gives us one way to define the *mean curvature*  $H$ : It measures the local increase (or decrease) in area as we move through the family of parallel surfaces. Explicitly, if  $d\sigma$  denotes the induced area form on  $\Sigma$  and  $d\sigma_t$  denotes the induced area form on  $\Sigma_t$  (and then pulled back to  $\Sigma$  via  $\Phi_t$ ), then the mean curvature  $H$  is defined to be the unique function on  $\Sigma$  such that

$$\frac{\partial}{\partial t} \Big|_{t=0} d\sigma_t = H d\sigma,$$

at each  $p \in \Sigma$ . Note that the sign of  $H$  will depend on choice of  $\nu$ . See Figure 8.

One can then show that for *any* outward normal variation with first-order variation  $X = e^u \nu$ , we have  $\frac{\partial}{\partial t} \Big|_{t=0} d\sigma_t = e^u H d\sigma$ . From this we see that if  $H > 0$  on  $\Sigma$ , then all small outward normal variations will increase area, and if  $H < 0$  on  $\Sigma$ , then all small outward normal variations will decrease area. A *minimal surface* is defined to be a surface with  $H = 0$  everywhere. It is called this because any surface whose area minimizes area among all small outward and inward normal variations must have  $H = 0$ . (Note that it is a bit of a misnomer since a minimal surface need not minimize area among variations.)

Now consider a spacelike 2-surface  $\Sigma$  in a 4-dimensional spacetime  $(N, g)$ . Now, instead of having a 1-dimensional space of normal vectors at each point of  $\Sigma$ , we have a 2-dimensional space of normal vectors. However, our spacetime geometry picks out exactly two future *null* directions, which correspond to two normal directions from which light rays can originate. Specifically, if  $\nu$  is a spacelike unit vector orthogonal to  $\Sigma$  and  $e_0$  is a future timelike unit vector orthogonal to both  $\Sigma$  and  $\nu$ , then those two future null directions are given by  $e_0 + \nu$  and  $e_0 - \nu$ . Suppose that  $\ell$  is a future null vector field defined along  $\Sigma$  which is normal to  $\Sigma$  at each point. Note that we cannot demand a “unit length” normalization since  $\ell$  has “length” zero. Multiplying  $\ell$  by a positive function yields another future null normal vector field defined along  $\Sigma$ , but modulo this sort of rescaling, there can only be two choices of future null normal, and we may designate one of them as “outward.” Given a choice of (future) outward null normal  $\ell$  for  $\Sigma$ , we use it in the following construction:

Define a family  $\Sigma_t = \Phi_t(\Sigma)$  in  $N$  by defining  $\Phi_t(p) = \exp_p(t\ell)$ , where  $\exp_p$  is the exponential map at  $p$ . This is the family of “light shells” referred to in Section 2, and it is analogous to the family of parallel surfaces in the Riemannian setting. Now we define the *(outward) null expansion* analogously to how we defined the mean curvature: It is the unique function  $\theta$  on  $\Sigma$  with the property that

$$\frac{\partial}{\partial t} \Big|_{t=0} d\sigma_t = \theta d\sigma$$

at each  $p \in \Sigma$ . Since  $\theta$  depends on the exact choice of  $\ell$ , and there is no natural choice of scaling for  $\ell$ , it turns out that only the sign of  $\theta$  is a physical or geometric property of  $\Sigma$ . We can now define  $\Sigma$  to be an *(outer) trapped surface* if  $\theta < 0$ , an *(outer) untrapped surface* if  $\theta > 0$ , or a *marginally outer trapped surface* (or MOTS) if  $\theta = 0$ .

Now suppose that the 2-surface  $\Sigma$  lies in a designated spacelike slice  $M$  of the spacetime  $(N, g)$ . In this case, a choice of outward normal  $\nu$  to  $\Sigma$  in  $M$  gives us a choice of outward null normal  $\ell$  on  $\Sigma$  by taking  $\ell = e_0 + \nu$  as above, where  $e_0$  is the future timelike unit normal to  $M$ . In the

special case where  $M$  is totally geodesic in  $N$ ,  $\theta$  is equal to  $H$ , and hence a MOTS is just a minimal surface. Because of this, MOTS can be thought of as generalizations of minimal surfaces, and therefore any general facts or heuristics about MOTS arising from physics automatically translate into statements about minimal surfaces. Conversely, some parts of the highly developed theory of minimal surfaces can be used to attack questions concerning MOTS. For example, the existence theory for minimal surfaces using barriers was adapted by Lars Andersson and Jan Metzger and by Michael Eichmair to prove a corresponding existence theorem for MOTS, and they were also able to prove that an apparent horizon must be a smooth MOTS [AEM11].

## 5. Topology of Black Holes

Going back to the example of the Schwarzschild spacetime, each choice of  $(v, r)$  defines a 2-sphere  $\Sigma_{v,r}$ . In this case, there is a natural choice for which of the two future null directions is “outward” and we can choose it as our  $\ell$ , and then we can compute the null expansion  $\theta$  of  $\Sigma_{v,r}$  to see that  $\Sigma_{v,r}$  is trapped when  $r < 2m$ , untrapped when  $r > 2m$ , and is a MOTS when  $r = 2m$ . See Figure 7. In fact, one can show that for a spacelike slice  $M$  of Schwarzschild, the apparent horizon in  $M$  is actually equal to the intersection of  $M$  with the event horizon. More generally, this is true for any slice  $M$  of a “stationary” spacetime.<sup>3</sup> Using this fact, Hawking was able to show, under reasonable physical hypotheses, that any cross-section (*i.e.* a spacelike 2-surface) of an event horizon in a stationary spacetime must be a topological sphere [Haw72]. Or in simpler terms, the surface of a black hole must be a topological sphere. Based on a suggestion by Gary Gibbons, Hawking was able to generalize his argument to show that even without the stationary hypothesis (which is very strong), apparent horizons must be topological spheres [Haw73]. We will explain this result below.

Let  $M$  be a spacelike slice of a spacetime. Given a surface  $\Sigma$  in  $M$  with a choice of “outward” normal  $\nu$ , we say that  $\Sigma$  is a *locally outermost MOTS in  $M$*  if it is a MOTS and there do not exist arbitrarily small outward normal variations of  $\Sigma$  in  $M$  with  $\theta \leq 0$ . An apparent horizon in  $M$  must be a locally outermost MOTS in  $M$ , and this is the relevant property used in Hawking’s proof, which is a beautiful combination of calculus of variations and the Gauss-Bonnet theorem.

**Theorem 1** (Hawking). *Any orientable locally outermost closed MOTS in an initial data set satisfying the dominant energy condition must be a topological sphere.*

<sup>3</sup>A spacetime is called stationary if it admits a global Killing vector field that is asymptotically timelike.

The dominant energy condition is a physically realistic assumption on the stress-energy tensor<sup>4</sup>, which we will come back to later. This result was generalized by Gregory Galloway and Schoen, who showed that higher dimensional analogues of apparent horizons must be topologically Yamabe positive [GS06].

## 6. The Locally Outermost Property

Schoen and Yau were the first to notice that minimal surfaces could be used to study scalar curvature. The *scalar curvature*  $R_M$  of a Riemannian metric  $(M, g)$  is a scalar function on  $M$  which is defined to be the full trace of the Riemann curvature tensor of  $g$ , and as its name suggests, it is the simplest scalar function that can be computed from  $g$  that is invariant under change of coordinates. In three dimensions, it has the property that for small  $r > 0$ , the volume of the geodesic ball of radius  $r$  around  $p \in M$  is given by  $\frac{4}{3}\pi r^3 - \frac{2\pi}{45}R_M(p)r^5 + O(r^7)$ , so  $R_M(p)$  measures the deviation of volumes of small balls around  $p$  from their Euclidean comparison balls. A similar formula holds in other dimensions, and in particular, for a 2-surface  $\Sigma$ ,  $R_\Sigma$  is just twice the more familiar Gauss curvature  $K_\Sigma$ .

While Hawking exploited the relationship between an outermost MOTS  $\Sigma$ , the dominant energy condition, and the Gauss curvature of  $\Sigma$ , Schoen and Yau similarly exploited the relationship between an area minimizing surface  $\Sigma$ , scalar curvature of the ambient Riemannian space, and the Gauss curvature of  $\Sigma$ . To be more precise, suppose we have a closed orientable surface  $\Sigma$  in a Riemannian 3-manifold with nonnegative scalar curvature. Schoen and Yau observed that if  $\Sigma$  minimizes area compared to all small variations of  $\Sigma$ , then  $\Sigma$  must be topologically either a sphere or a torus. By a refined argument, Mingliang Cai and Galloway showed that if  $\Sigma$  is *strictly* area-minimizing, then  $\Sigma$  must be a topological sphere. We will explain a similar result that is a special case of Hawking’s theorem.

Given a surface  $\Sigma$  with a choice of “outward” normal  $\nu$ , we will say that  $\Sigma$  is a *locally outermost minimal surface* if it is a minimal surface and there are no arbitrarily small outward normal variations of  $\Sigma$  with  $H \leq 0$ .

**Theorem 2.** *Any orientable locally outermost closed minimal surface  $\Sigma$  in a Riemannian 3-manifold  $(M, g)$  with nonnegative scalar curvature must be a topological sphere.*

*Proof.* Let  $\Sigma_t$  be an outward normal variation of  $\Sigma$  in  $M$ , with first-order variation  $X = e^u\nu$ , and let  $H_t$  denote the mean curvature of  $\Sigma_t$  (pulled back to  $\Sigma$ ). One can always

<sup>4</sup>Explicitly, we say that an initial data set  $(M, g, k)$  satisfies the dominant energy condition if the Einstein tensor satisfies  $\mathbf{G}(e_0, v) \geq 0$  where  $e_0$  is the future normal to  $M$  and  $v$  is any future null or timelike vector. The condition can also be expressed purely in terms of  $(g, k)$ .

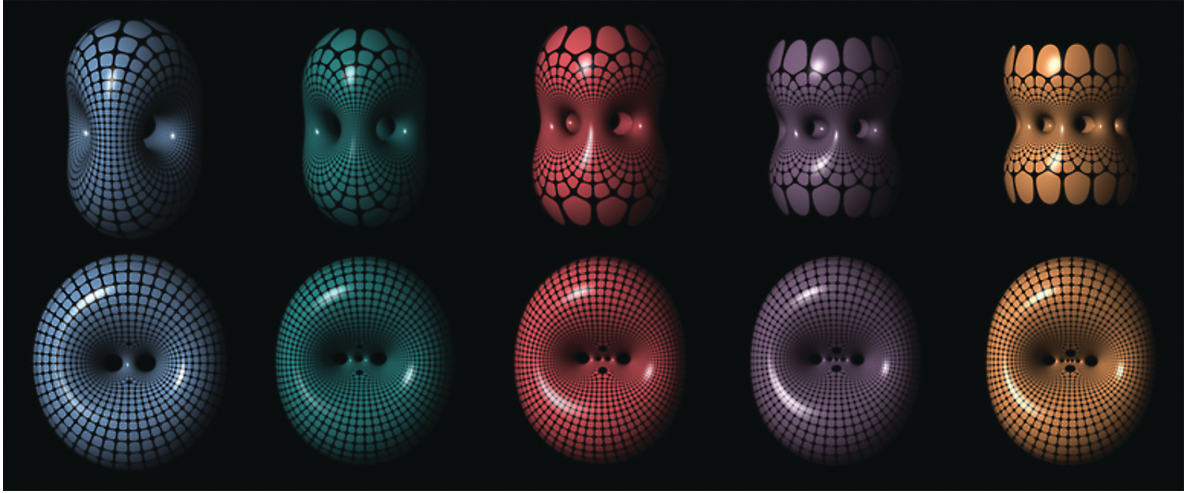


**Figure 9.** Lawson's minimal surfaces of genus 2, 3, 4, 5, and 6 in  $S^3$ , stereographically projected to  $\mathbb{R}^3$  in two different ways.

find an outward normal variation such that

$$\frac{\partial H_t}{\partial t} \Big|_{t=0} = \lambda e^u \quad (1)$$

for some constant  $\lambda$ . (More precisely,  $e^u$  is chosen to be the principal eigenfunction of the linearized mean curvature operator.) The locally outermost assumption on  $\Sigma$  implies that  $\lambda \geq 0$ , because otherwise, we would have  $H_t < 0$  for small  $t > 0$ .

Routine geometric computations, including use of the Gauss equation, show that

$$\begin{aligned} \frac{\partial H_t}{\partial t} \Big|_{t=0} &= e^u \left( -\Delta_\Sigma u - |\nabla u|^2 + K_\Sigma - \frac{1}{2} R_M - \frac{1}{2} |A|^2 \right) \\ &\leq e^u (-\Delta_\Sigma u + K_\Sigma), \end{aligned} \quad (2)$$

where  $\Delta_\Sigma$  denotes the Laplace-Beltrami operator on  $\Sigma$ ,  $A$  is the second fundamental form of  $\Sigma$  in  $M$ , and we used the assumption that  $R_M \geq 0$ . Combining this with (1), we have

$$\lambda \leq -\Delta_\Sigma u + K_\Sigma,$$

and integrating this over  $\Sigma$  and using the Gauss-Bonnet Theorem, it follows that

$$0 \leq \lambda \cdot (\text{Area } \Sigma) \leq 2\pi\chi(\Sigma).$$

Therefore  $\Sigma$  is either a torus or a sphere.

To rule out the torus, suppose to the contrary that  $\Sigma$  is a torus. Then  $\chi(\Sigma) = 0$ , and thus  $\lambda = 0$ . In this case, an inverse function theorem argument can be used to construct an outward normal variation  $\Sigma_t$  with the added property that each  $\Sigma_t$  has *constant* mean curvature  $H_t$ . Let  $X_t = e^{u_t} \nu_t$  be the first-order variation of  $\Sigma_t$  at an arbitrary  $t$ . As in (2), we have

$$\frac{\partial H_t}{\partial t} e^{-u_t} \leq -\Delta_{\Sigma_t} u_t + K_{\Sigma_t}.$$

Since  $\Sigma_t$  is a torus and  $\frac{\partial H_t}{\partial t}$  is constant over  $\Sigma_t$ , integrating both sides of the above inequality over  $\Sigma_t$  shows that  $\frac{\partial H_t}{\partial t} \leq 0$  for all  $t \geq 0$ , which contradicts the locally outermost assumption.  $\square$

Without the locally outermost assumption, a minimal surface can have higher genus. For example, the standard 3-sphere admits closed minimal surfaces of arbitrary genus. See Figure 9. Over the last decade Fernando Marques and André Neves have advanced the study of minimal surfaces using min-max methods, and building on their work, Haozhao Li and Xin Zhou proved that a generic closed Riemannian 3-manifold with positive Ricci curvature admits closed minimal surfaces with arbitrarily high genus, and Antoine Song proved Yau's 1982 conjecture that all closed Riemannian 3-manifolds admit infinitely many closed minimal surfaces.

The proof of Theorem 1 is conceptually similar to that of Theorem 2. In that case, we start with an orientable locally outermost closed MOTS  $\Sigma$  in an initial data set  $(M, g, k)$ . We still look at outward normal variations of  $\Sigma$  in  $M$ , but instead of (2), we obtain

$$\frac{\partial \theta_t}{\partial t} \Big|_{t=0} \leq e^u (-\Delta_\Sigma u + K_\Sigma + \text{div}_\Sigma W),$$

for some quantity  $W$ , where this time the inequality follows from the dominant energy condition rather than non-negative scalar curvature. The rest of the proof is essentially the same since the integral of the extra divergence term is zero. However, dealing with the case where  $\frac{\partial \theta_t}{\partial t} \Big|_{t=0} = 0$  requires an additional argument (by Galloway) because the formula for  $\frac{\partial \theta_t}{\partial t}$  at a general  $t$  has an extra term involving  $\theta_t$  (which happens to vanish when  $t = 0$ ).

## 7. Positive Mass Theorem

We will now discuss how a version of the topological argument from the previous section can be used to prove the celebrated positive mass theorem. Let  $(M, g, k)$  be an initial data set and assume that it is *asymptotically flat*, meaning that in coordinates, the metric  $g_{ij}$  is asymptotic to the Euclidean metric  $\delta_{ij}$  while the second fundamental form  $k_{ij}$  is asymptotic to zero, in some precise sense that we will not describe here. An asymptotically flat initial data set has a well-defined total *ADM energy-momentum*<sup>5</sup>  $(E, P_1, P_2, P_3)$ .

**Theorem 3** (Positive mass theorem). *Let  $M$  be a complete asymptotically flat 3-dimensional initial data set satisfying the dominant energy condition. Then the ADM energy-momentum  $(E, P_1, P_2, P_3)$  satisfies  $E \geq |P|$ . Furthermore, the equality  $E = |P|$  holds if and only if  $(M, g)$  can be isometrically embedded into the Minkowski spacetime with second fundamental form  $k$ .*

This is called the “positive mass theorem” because an object with future timelike energy-momentum  $E > |P|$  is said to have positive mass. Explicitly, the mass is  $\sqrt{E^2 - |P|^2}$ . Note that a spacelike slice of the Schwarzschild spacetime with mass  $m$  will (unsurprisingly) have ADM mass equal to  $m$ . Negative mass, which is unphysical, would correspond to past timelike energy momentum  $E < -|P|$ , while spacelike energy momentum  $|E| < |P|$ , which would correspond to “imaginary mass,” is also unphysical since it is associated with objects moving faster than the speed of light. Meanwhile, null energy-momentum  $|E| = |P|$  corresponds to zero mass.

The positive mass theorem is highly desirable for physical reasons. The dominant energy condition can be described as the reasonable physical assumption that the sources for Einstein’s equations cannot travel faster than light, as measured by any observer. The positive mass theorem loosely asserts that as long as these sources cannot travel faster than light, the entire configuration of sources, as viewed from far away, should not behave like an object traveling faster than light, or as fast as light. An example of a violation of the positive mass theorem could be a configuration of positive mass sources that somehow *repels* far away objects instead of attracting them. Because of the nonlinearities of Einstein’s equations, it is highly non-trivial to prove that such perversities cannot happen.

The study of the positive mass theorem has a long history. A particularly important special case is when  $M$  is

<sup>5</sup>The ADM energy-momentum was formulated by physicists Arnowitt, Deser, and Misner, and explicitly, the numbers  $(E, P_1, P_2, P_3)$  are defined by

$$16\pi E = \lim_{r \rightarrow \infty} \int_{|x|=r} \sum_{i,j} \left( \frac{\partial g_{ij}}{\partial x_i} - \frac{\partial g_{ii}}{\partial x_j} \right) \frac{x_j}{r} d\sigma,$$

$$8\pi P_i = \lim_{r \rightarrow \infty} \int_{|x|=r} \sum_j (k_{ij} - (\text{tr} k) g_{ij}) \frac{x_j}{r} d\sigma.$$

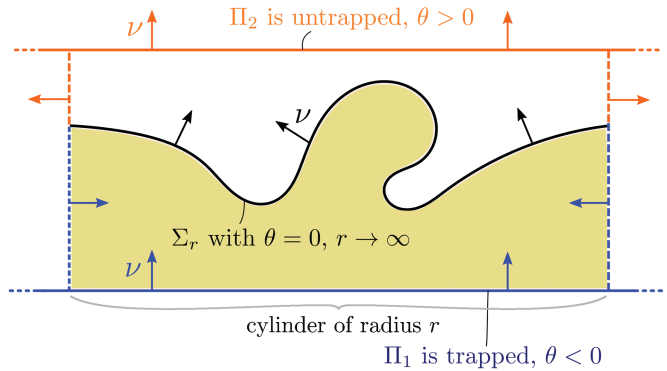


**Figure 10.** Under the (contradictory) assumption  $E < |P|$ , two coordinate planes  $\Pi_1$  and  $\Pi_2$ , together with the lateral side of a cylinder of large radius, provide barriers for the existence of a MOTS  $\Sigma_r$  with prescribed boundary. A subsequent limit surface of  $\Sigma_r$  as  $r \rightarrow \infty$  is a complete MOTS satisfying a stability property.

a totally geodesic slice of the spacetime. In this case, the positive mass theorem reduces to a statement about Riemannian geometry, which is often called the Riemannian positive mass theorem: If  $(M, g)$  is a complete asymptotically flat manifold with nonnegative scalar curvature, then  $E > 0$  unless  $(M, g)$  is Euclidean. This special case was first proved by Schoen and Yau in 1979 using minimal surfaces, and soon later they proved that  $E \geq 0$  in the general case using the Jang equation [SY79, SY81]. Edward Witten was able to prove that  $E \geq |P|$  using a spinor argument [Wit81]. This might be more accurately called a “nonnegative mass theorem” since it does not handle the second statement about  $E = |P|$  in Theorem 3, which we will refer as the *equality case of the positive mass theorem*. In a 2015 article with Eichmair and Schoen, we gave an alternative proof of this nonnegative mass theorem by extending Schoen and Yau’s argument and by replacing the minimal surfaces by MOTS [EHL16]. In that article we also tackled the more technically challenging case of  $n$ -dimensional slices, for  $3 < n < 8$ , by introducing a new functional that mimics the first variation of the area functional. There are recent results of Schoen and Yau and of Lohkamp that deal with higher dimensions. One can also weaken the hypotheses of Theorem 3 to allow  $M$  to have a boundary as long as that boundary is a closed trapped surface or MOTS [GHH83, LLU21]. Physically, this corresponds to allowing for the possibility of a black hole without having to assume too much about the geometry inside the black hole.

We outline the proof of the nonnegative mass theorem for 3-dimensional  $M$ .

*Outline of proof.* By a subtle density theorem (see Section 6 of [EHL16]), one can show that without loss of generality, we can assume that the “strict” dominant energy condition

holds and that the initial data  $(g, k)$  has especially “nice” asymptotics at spatial infinity.

The proof proceeds by contradiction. Suppose that  $E < |P|$ . The “nice” asymptotics imply that there exist non-intersecting coordinate planes  $\Pi_1$  and  $\Pi_2$  such that  $\Pi_1$  is trapped and  $\Pi_2$  is untrapped; namely,  $\theta < 0$  on  $\Pi_1$  and  $\theta > 0$  on  $\Pi_2$ . See Figure 10. From a PDE perspective, this means that they provide barriers for the MOTS equation  $\theta = 0$ . Using these barriers, an existence theorem due to Eichmair [Eic09] allows us to construct a MOTS with prescribed boundary that is sandwiched between the planes  $\Pi_1$  and  $\Pi_2$ . By taking that prescribed boundary larger and larger, we can extract a subsequential limit surface which is a complete MOTS  $\Sigma$  sandwiched between  $\Pi_1$  and  $\Pi_2$ , and we can show that  $\Sigma$  itself is asymptotically planar. While this  $\Sigma$  need not be a locally outermost MOTS, it still enjoys a “MOTS stability” property that, together with the strict dominant energy condition, can be used to show that  $\int_{\Sigma} K_{\Sigma} d\sigma > 0$  in a manner that is conceptually similar to the proof of Theorem 2. The “strict” dominant energy condition is what forces this inequality to be strict. Finally, the Gauss-Bonnet Theorem with boundary implies that this is impossible for an asymptotically planar surface.  $\square$

To prove the equality case of the positive mass theorem requires significant extra work. One must show that if  $E = |P|$ , then the slice  $M$  actually sits inside the Minkowski spacetime, in the sense described in the theorem. This actually implies that  $E = |P| = 0$  since any slice of Minkowski has this property. The equality case was proved for all spin manifolds by work of Robert Beig and Piotr Chruściel [BC96], and Chruściel and Daniel Maerten. This covers all 3-manifolds since all 3-manifolds carry spin structures. More recently, we were able to provide a separate proof that avoids the use of a spin assumption [HL20b]. Our proof uses a variational argument among initial data sets satisfying the dominant energy condition, which turns out to have an intriguing connection to the question of “improving” the dominant energy condition studied by Justin Corvino and the first author [CH20]. The improvability of the dominant energy condition manifestly relates to the fundamental problem of scalar curvature deformation in differential geometry and was further explored in our recent work [HL20a].

One curious feature of both our proof and the spinor proof is that in higher dimensions, the equality case of the positive mass theorem seems to require a stronger definition of asymptotic flatness than the standard one needed for the “nonnegative mass theorem” to be true. Somewhat surprisingly, it turns out that when the spatial dimension is greater than eight, there do exist counterexamples to the expected strict inequality  $E > |P|$ . See Example 7 of [HL20a]. Those examples arise from an important family of exact solutions to the Einstein equations, called

plane-fronted waves with parallel rays (or *pp-waves* for short), which model radiation moving at the speed of light, and thus any spacelike slices naturally have  $E = |P|$  (so long as these quantities can be defined). The counterexamples come from slices of pp-waves which are asymptotically flat enough to satisfy the hypotheses of the nonnegative mass theorem, but not asymptotically flat enough to satisfy the hypotheses of the equality case of the positive mass theorem.

While Penrose’s advances were only recently honored by the Nobel Prize in Physics, the topological and geometric methods that he introduced helped to build a long, intimate relationship between mathematics and general relativity over the past several decades. We discussed groundbreaking work of Hawking, Schoen, and Yau as fine examples of the intriguing interactions between geometry, topology, analysis, and general relativity. New applications and interconnections between mathematics and general relativity are continually being discovered in more recent developments, as described above. For a more extensive introduction to this field of research, please see the recent graduate-level textbook by the second author [Lee19]. We expect that the exchange of ideas between physics and mathematics will continue to energize these directions of inquiry, which we have only lightly touched upon here. Penrose once stated, “We have a closed circle of consistency here: the laws of physics produce complex systems, and these complex systems lead to consciousness, which then produces mathematics, which can then encode in a succinct and inspiring way the very underlying laws of physics that gave rise to it.”

## References

- [AEM11] Lars Andersson, Michael Eichmair, and Jan Metzger, *Jang’s equation and its applications to marginally trapped surfaces*, Complex analysis and dynamical systems IV. Part 2, Contemp. Math., vol. 554, Amer. Math. Soc., Providence, RI, 2011, pp. 13–45, DOI 10.1090/conm/554/10958. MR2884392
- [BC96] Robert Beig and Piotr T. Chruściel, *Killing vectors in asymptotically flat space-times. I. Asymptotically translational Killing vectors and the rigid positive energy theorem*, J. Math. Phys. 37 (1996), no. 4, 1939–1961, DOI 10.1063/1.531497. MR1380882
- [CH20] Justin Corvino and Lan-Hsuan Huang, *Localized deformation for initial data sets with the dominant energy condition*, Calc. Var. Partial Differential Equations 59 (2020), no. 1, Paper No. 42, 43, DOI 10.1007/s00526-019-1679-9. MR4062040
- [EG96] A. Eckart and R. Genzel, *Observations of stellar proper motions near the galactic centre*, Nature 383 (1996), no. 6599, 415–417.
- [Eic09] Michael Eichmair, *The Plateau problem for marginally outer trapped surfaces*, J. Differential Geom. 83 (2009), no. 3, 551–583. MR2581357

[EHLS16] Michael Eichmair, Lan-Hsuan Huang, Dan A. Lee, and Richard Schoen, *The spacetime positive mass theorem in dimensions less than eight*, J. Eur. Math. Soc. (JEMS) **18** (2016), no. 1, 83–121, DOI 10.4171/JEMS/584. MR3438380

[Eve19] Event Horizon Telescope Collaboration, *First M87 Event Horizon Telescope Results. I. The Shadow of the Supermassive Black Hole*, ApJL **875** (April 2019), no. 1, L1, available at 1906.11238.

[GS06] Gregory J. Galloway and Richard Schoen, *A generalization of Hawking’s black hole topology theorem to higher dimensions*, Comm. Math. Phys. **266** (2006), no. 2, 571–576, DOI 10.1007/s00220-006-0019-z. MR2238889

[GKMB98] A. M. Ghez, B. L. Klein, M. Morris, and E. E. Becklin, *High Proper-Motion Stars in the Vicinity of Sagittarius A\*: Evidence for a Supermassive Black Hole at the Center of Our Galaxy*, ApJ **509** (December 1998), no. 2, 678–686, available at astro-ph/9807210.

[GHHP83] G. W. Gibbons, S. W. Hawking, Gary T. Horowitz, and Malcolm J. Perry, *Positive mass theorems for black holes*, Comm. Math. Phys. **88** (1983), no. 3, 295–308. MR701918

[Haw72] S. W. Hawking, *Black holes in general relativity*, Comm. Math. Phys. **25** (1972), 152–166. MR293962

[Haw73] S. W. Hawking, *The event horizon*, Les Houches Summer School of Theoretical Physics: Black Holes, 1973.

[HL20a] Lan-Hsuan Huang and Dan A. Lee, *Bartnik mass minimizing initial data sets and improvability of the dominant energy scalar*, arXiv:2007.00593 [math.DG] (2020).

[HL20b] Lan-Hsuan Huang and Dan A. Lee, *Equality in the spacetime positive mass theorem*, Comm. Math. Phys. **376** (2020), no. 3, 2379–2407, DOI 10.1007/s00220-019-03619-w. MR4104553

[Lee19] Dan A. Lee, *Geometric relativity*, Graduate Studies in Mathematics, vol. 201, American Mathematical Society, Providence, RI, 2019. MR3970261

[LLU21] Dan A. Lee, Martin Lesourd, and Ryan Unger, *Density and positive mass theorems for initial data sets with boundary*, arXiv:2112.12017 [math.DG] (2021).

[Pen65] Roger Penrose, *Gravitational collapse and space-time singularities*, Phys. Rev. Lett. **14** (1965), 57–59, DOI 10.1103/PhysRevLett.14.57. MR172678

[SY79] Richard Schoen and Shing Tung Yau, *On the proof of the positive mass conjecture in general relativity*, Comm. Math. Phys. **65** (1979), no. 1, 45–76. MR526976

[SY81] Richard Schoen and Shing Tung Yau, *Proof of the positive mass theorem. II*, Comm. Math. Phys. **79** (1981), no. 2, 231–260. MR612249

[Wit81] Edward Witten, *A new proof of the positive energy theorem*, Comm. Math. Phys. **80** (1981), no. 3, 381–402. MR626707



Lan-Hsuan Huang



Dan A. Lee

#### Credits

Opening image is courtesy of NASA’s Goddard Space Flight Center; background, ESA/Gaia/DPAC.

Figure 1 is courtesy of NASA, ESA, and D. Coe, J. Anderson, and R. van der Marel (STScI).

Figure 2 is courtesy of Left\_Coast\_Photographer.

Figure 3 is courtesy of NASA/JPL-Caltech/IPAC/Event Horizon Telescope Collaboration.

Figure 4 (left) is courtesy of arinahabich via Getty.

Figure 4 (right) is courtesy of Julián Norato, adapted from [ntopology.com](http://ntopology.com).

Figures 5–8 and 10 are courtesy of Lan-Hsuan Huang.

Figure 9 is courtesy of Nick Schmitt.

Photo of Lan-Hsuan Huang is courtesy of Damin Wu.

Photo of Dan A. Lee is courtesy of Dan A. Lee.

## AMS AUTHOR RESOURCE CENTER

The Author Resource Center is a collection of information and tools available to assist you to successfully write, edit, illustrate, and publish your mathematical works.

To begin utilizing  
these important  
resources, visit:

[www.ams.org/authors](http://www.ams.org/authors)



 **AMS** AMERICAN MATHEMATICAL SOCIETY  
Advancing research. Creating connections.